*Kinetics and Catalysis, Vol. 43, No. 6, 2002, pp. 838–846. Translated from Kinetika i Kataliz, Vol. 43, No. 6, 2002, pp. 902–911.*


# Effect of the Structure of Carbon Nanofibers on the State of an Active Component and on the Catalytic Properties of Pd/C Catalysts in the Selective Hydrogenation of 1,3-Butadiene

**V. V. Chesnokov, I. P. Prosvirin, N. A. Zaitseva, V. I. Zaikovskii, and V. V. Molchanov**

*Boreskov Institute of Catalysis, Siberian Division, Russian Academy of Sciences, Novosibirsk, 630090 Russia*

Received November 20, 2001

**Abstract**—The state of highly dispersed palladium particles supported on filamentous carbon was studied using high-resolution electron microscopy, XPS, and X-ray diffraction analysis. Three types of filamentous carbon were used, in which the basal planes of graphite were arranged along, across, and at an angle to the nanofiber axis. The amount of supported palladium was 0.25–5.8 wt %. The structure of the carbon support was found to affect the properties of the active component. Highly dispersed palladium particles exhibited the strongest interaction with a carbon surface formed by the butt ends of graphite (002) layers. This interaction resulted in electron transfer from the metal to the support and in the stabilization of palladium in the most dispersed state. A change in the properties of palladium particles caused a change in the catalytic properties of Pd/C catalysts in the reaction of selective 1,3-butadiene hydrogenation to butenes. The strong interaction of $Pd^{2+}$ with the butt ends of graphite resulted in the stabilization of palladium in an ionic state. An increase in the fraction of $Pd^{2+}$ in the catalysts was responsible for a decrease in both the overall activity and selectivity of Pd/C catalysts in the reaction of 1,3-butadiene hydrogenation to butenes.

## INTRODUCTION

Hydrogenation processes are widely used in industry for the removal of undesirable highly unsaturated impurities from various hydrocarbon fractions and individual substances. They should be selective, and the reaction should be terminated after the first step of hydrogenation. Palladium catalysts on carbon supports are effective in these processes [1–6]. Because of this, a considerable number of publications were devoted to studies of Pd/C catalysts [6–9]. In these studies, it was found that hydrogenation reactions are structure sensitive; that is, the reaction activity and selectivity depends on the size and the face type of catalytically active metal particles [9, 10]. If the chemical composition of a surface is constant, the metal particle size is responsible for the electronic structure of active centers, the interaction with reactants, and, ultimately, the catalytic properties of the system.

Moreover, the state of the metal is affected by the metal–carbon support interaction. In turn, this interaction depends on the surface structure of carbon. However, the effect of this interaction on the catalytic properties of Pd/C catalysts has been insufficiently studied because the structure of the carbon supports is complex and the possibilities of the synthesis of supports with specified properties are restricted. Recently, considerable progress in studies of the mechanisms of formation of filamentous carbon and control over its crystal structure has been achieved. In this work, we used filamentous carbon of types that are fundamentally different in structure as catalyst supports.

The aim of this work was to study the effect of the structure of filamentous carbon on the state of palladium and on the catalytic properties of Pd/C catalysts in the selective hydrogenation reaction of 1,3-butadiene.

## EXPERIMENTAL

Carbon nanofibers were prepared from hydrocarbons ($CH_4$ and $C_4H_6$) in a quartz flow reactor with the McBain balance under gradientless conditions in terms of temperature. Nickel-containing catalysts (0.02–0.2 g) were loaded into the setup; the sensitivity of mass measurements was $10^{-4}$ g. Methods for the preparation of filamentous carbon with different arrangements of graphite layers in the bodies of filaments were considered in more detail elsewhere [11].

The X-ray diffraction analysis of samples was performed on a D-500 diffractometer (Siemens). Monochromated Cu$K_\alpha$ radiation was used (a graphite monochromator on a reflected beam).

Carbon nanofibers and palladium particles supported on them were examined by high-resolution transmission electron microscopy in combination with electron diffraction on a JEM-2010 instrument with an accelerating voltage of 200 kV and a line resolution of 1.4 Å.

The dispersity of Pd/C catalysts was determined by a pulse method using CO chemisorption at 20°C in accordance with a published procedure [12].

Because samples that were used for growing nanofibers contained nickel metal or nickel–copper alloys, the resulting products contained from 0.5 to 15 wt %

0023-1584/02/4306-0838$27.00 

nickel. After etching in aqua regia, carbon nanofibers were analyzed for nickel and supported palladium by X-ray spectrum analysis on a VRA-20 analyzer with a W anode of the X-ray tube.

Both carbon supports and Pd/C catalysts were studied by XPS. All of the experiments were performed on a VG ESCALAB HP spectrometer with the use of unmonochromated Al$K_\alpha$ radiation ($h\nu$ = 1486.6 eV; 200 W). In the course of measuring the spectra, the residual gas pressure in the analyzer chamber was $5 \times 10^{-7}$ Pa.

The binding energy ($E_b$) scale of the spectrometer was precalibrated using the peak positions of the Au4$f_{7/2}$ (84.00 eV) and Cu2$p_{3/2}$ (932.67 eV) core levels. To remove the charging effect, test samples were rubbed into nickel gauze. The line of C1*s* with $E_b$ = 284.4 eV belonging to carbon contained in the support material was used as an internal standard.

The relative concentrations of elements on catalyst surfaces and the ratios between their atomic concentrations were determined from the integrated intensities of photoelectron lines corrected for the corresponding atomic sensitivity factors [13].

The reaction of butadiene hydrogenation was performed in a circulation flow setup at 60–150°C. The catalyst weight was 0.05 g; the flow rates of hydrogen and unsaturated hydrocarbons were 7 and 1.4 l/h, respectively. The reaction products were analyzed by chromatography. Zeolite NaX and triethylene glycol *n*-butyrate on diatomaceous earth were used as adsorbents.

Previously, based on studies of the formation of a graphite phase from carbon atoms formed on the degradation of hydrocarbons on iron subgroup metals by the carbide cycle mechanism, methods were developed for the controlled preparation of the main structures of graphite nanofibers (Fig. 1). Filamentous carbon offers outstanding possibilities in controlling the crystallographic structure of the surface of a carbon support. Earlier [11], three fundamentally different types of filamentous carbon were prepared, in which the basal planes of graphite were arranged along, across, and at an angle to the filament axis, that is, coaxially cylindrical, stacklike, and coaxially conical carbon nanofibers. The structure of stacklike filamentous carbon can be represented as a great number of graphite basal planes arranged in a stack. Only the butt-end faces of graphite occur at the outer surface of a nanofiber. The unsaturation of carbon atom bonds at the butt-end faces is very high, so that carbon layers are closed on each other at some sites of a nanofiber [14].

To prepare a pure carbon material, metal particles, which catalyzed the growth of filamentous carbon, were etched from the samples using aqua regia. However, the boiling of carbon nanofibers in aqua regia for several hours did not fully remove nickel from the samples; this can be explained by the partial blocking of the metal with carbon. Table 1 summarizes the residual nickel contents of carbon nanofibers after etching.

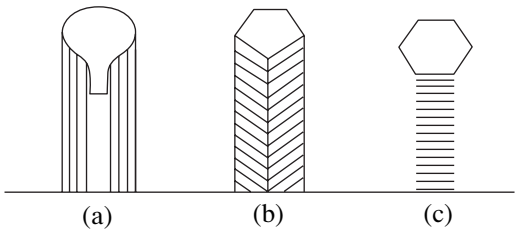


**Fig. 1.** Schematic diagram of the longitudinal sections of the main types of carbon nanofibers. Spatial arrangements of the basal planes of graphite: (a) coaxially cylindrical, (b) coaxially conical, and (c) stacklike.

The blocking of nickel metal with carbon was supported by electron-microscopic studies and data on the catalytic activity of carbon nanofibers in the reaction of 1,3-butadiene hydrogenation. We experimentally found that carbon nanofibers exhibited no catalytic activity in 1,3-butadiene hydrogenation at 20–150°C.

After etching, palladium was supported on all of the three types of carbon nanofibers from aqueous $PdCl_2$ solutions. Table 2 summarizes the palladium contents of the samples.

## RESULTS AND DISCUSSION

### *X-ray Diffraction Analysis of Pd/C Catalysts*

With the use of X-ray diffraction analysis, we found that all of the carbon nanofibers consisted of differently ordered graphite. The X-ray diffraction patterns exhibited an intense line of graphite at an angle of ~26° (2θ); this line corresponded to $d_{002}$ = 3.39–3.44 Å depending on the type of carbon nanofibers (Table 3). Nickel was not detected by X-ray diffraction analysis in the samples of nanofibers with coaxially conical and stacklike structures after etching in aqua regia. The X-ray diffraction patterns of the filamentous carbon with the coaxially cylindrical structure exhibited weak lines that are characteristic of nickel.

The graphite lattice parameters remained unchanged after the impregnation of carbon supports with coaxially cylindrical and coaxially conical structures with an aqueous $PdCl_2$ solution followed by drying at 100°C. They also remained unchanged after the

**Table 1.** Nickel contents of carbon nanofibers after etching in aqua regia

| Type of carbon nanofibers | Ni content, wt % |
|---|---|
| Stacklike | 0.5 |
| Coaxially conical | 0.9 |
| Coaxially cylindrical | 6.1 |

**Table 2.** Palladium contents of Pd/C catalysts

| Sample no. | Type of filamentous carbon | Pd content, wt % |
|---|---|---|
| 1205 | Stacklike | 0 |
| 2030 | Stacklike | 0.25 |
| 1742 | Stacklike | 0.50 |
| 1848 | Stacklike | 2.50 |
| 1850 | Stacklike | 5.80 |
| 1827 | Coaxially conical | 0.58 |
| 1841 | Coaxially conical | 3.15 |
| 2031 | Coaxially cylindrical | 0.25 |
| 1818 | Coaxially cylindrical | 0.60 |
| 1842 | Coaxially cylindrical | 2.62 |

**Table 3.** Properties of filamentous carbon according to X-ray diffraction analysis

| Carbon nanofibers | Nanofiber preparation temperature, °C | Graphite lattice parameter, Å | Coherent-scattering region, Å |
|---|---|---|---|
| Coaxially conical | 500 | 3.44 | 50 |
| Stacklike | 600 | 3.40 | 65 |
| Coaxially cylindrical | 750 | 3.39 | 140 |

reduction of Pd/C catalysts at 250°C. In the case of the filamentous carbon with the stacklike structure, the graphite lattice parameter $d_{002}$ increased by 0.1 Å, regardless of the amount of supported palladium, after impregnation with an aqueous $PdCl_2$ solution and subsequent drying at 100°C. However, after the reduction of Pd/C catalysts of this type at 250°C, the graphite lattice parameter decreased to the initial value. These data suggest that both solvent ions and $Pd^{2+}$ and $Cl^-$ ions can enter the interlayer space of graphite.

### *XPS Study of Pd/C Catalysts*

The chemical composition of Pd/C samples was determined by the XPS method. The chemical shifts of core levels were correlated, and the occurrence of chemical bonds and the oxidation states of palladium were assumed.

The presence of chlorine, carbon, oxygen, and palladium was detected in all samples. No additional impurities were detected to within the sensitivity of XPS. The XPS method provides information on the state of a surface layer at a depth of 25–30 Å. The fact that nickel was not detected by XPS provides support for the blocking of nickel particles with carbon.

Note that the intensity of the Pd3*d* line in the survey spectra of samples containing 0.5% palladium was very low; because of this, a considerable time was required to accumulate a useful signal in the Pd3*d* spectrum.

Figure 2 demonstrates the C1*s* spectra of Pd/C samples prepared using a carbon support (sample no. 1205; carbon nanofibers with the stacklike structure).

An analysis of the above spectra allowed us to conclude that the C1*s* peak with the binding energy 284.4 eV (peak half-width of about 1.5–1.55 eV) is characteristic of all samples. The shape of the C1*s* peak is somewhat asymmetric: a shoulder is observed at higher binding energies. This shoulder can be due to the occurrence of C–Cl and C–O bonds at the surface of the carbon support. The carbon peak intensity insignificantly changed from sample to sample; subsequently, all photoelectron peaks were normalized to the peak (C1*s*) of carbon (sample no. 1205). All of the other spec-

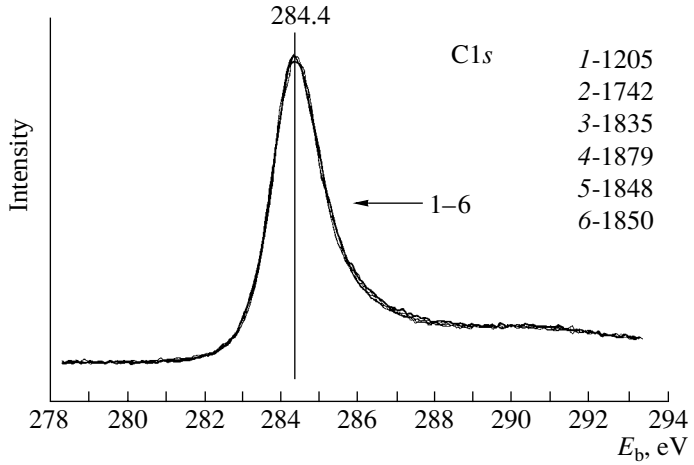


**Fig. 2.** XPS C1*s* spectra of Pd/C samples.

tra considered in this work were normalized in a similar manner.

Figure 3 demonstrates the Cl2*p* spectra. The binding energies of the Cl2*p* line were similar in all samples and equal to 200.1 eV. The line with the peak maximum at 200.1 eV can be attributed to chlorine atoms bound to the carbon of the support. The intensities of chlorine peaks in sample nos. 1205 (support) and 1742 (Pd/C catalyst after supporting $PdCl_2$ and drying at 100°C) were similar. The Pd/C catalyst sample (no. 1742) exhibited a shoulder at lower binding energies with the peak maximum at 198.0–194.4 eV, which can be attributed to α-$PdCl_2$ [15]. This also results in a somewhat higher Cl : C concentration ratio in sample no. 1742 as compared with that in sample no. 1205 (Table 4).

The Cl : C ratio decreased on the subsequent reduction of Pd/C catalysts in hydrogen at 250 (sample no. 1835; 0.5% Pd/C) and 300°C (sample no. 1879; 0.5% Pd/C) by factors of 3.3 and 5, respectively, as compared with catalyst no. 1742 (0.5% Pd/C after drying). Palladium chloride gives palladium metal upon reduction. Figure 4 demonstrates the photoelectron spectra of the Pd3*d* level.

An analysis of the spectra shown in Fig. 4 demonstrates that the Pd3*d* spectrum of sample no. 1742 exhibits two states of palladium: the main peak with the binding energy 337.4 eV and a shoulder at lower binding energies (336.4 eV). The binding energy of the main peak equal to 337.4 eV, which is close to that of compounds that have a bond between chlorine and palladium, and a shoulder at lower binding energies for the

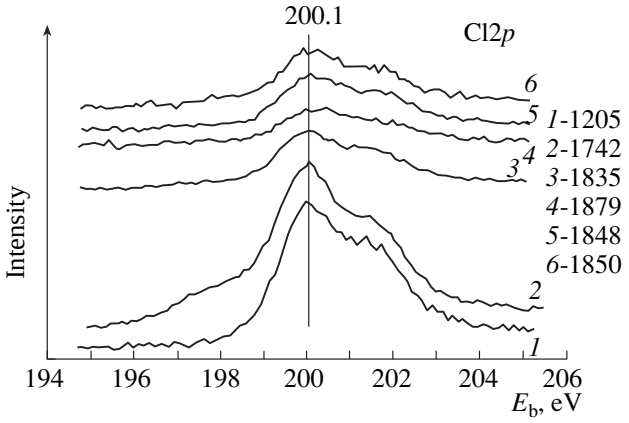


**Fig. 3.** XPS Cl2*p* spectra of Pd/C samples.

Cl2*p* line (198.2–198.5 eV), which corresponds to chlorine in the compound $PdCl_2$, allowed us to attribute this peak to palladium chloride ($PdCl_2$), which is present at the sample surface after the stages of impregnation and drying. It follows from published data that palladium metal $Pd^0$ is characterized by $E_b$ = 335.3 eV. For small clusters (<20–30 Å), a shift in the binding energy of the core level and a narrowing of the valence band with respect to the bulk metal are observed [16–20]. It was found that the binding energies of core levels increased with decreasing number of atoms in a cluster. In highly dispersed Pd/C catalysts, the shift of the binding energy of the core level was 1.0–1.3 eV. Thus, the shoulder with $E_b$ = 336.4 eV corresponds to highly dis-

**Table 4.** Atomic concentration ratios between the elements in Pd/C samples

| Sample no. | Pd, wt % | $T_{red}$, °C | Atomic concentration ratio | | | | |
|---|---|---|---|---|---|---|---|
| | | | Pd/C | Pd/Cl | Pd/O | O/C | Cl/C |
| 1205 | 0 | – | – | – | – | 0.054 | 0.025 |
| 1742 | 0.5 | Unreduced | 0.0014 | 0.034 | 0.020 | 0.055 | 0.037 |
| 1835 | 0.5 | 250 | 0.0012 | 0.110 | 0.024 | 0.049 | 0.011 |
| 1879 | 0.5 | 300 | 0.0012 | 0.180 | 0.028 | 0.044 | 0.0069 |
| 2007 | 0.5 | 250 ($T_{calcd}$ = 450) | 0.0011 | 0.230 | 0.031 | 0.037 | 0.0051 |
| 2008 | 0.5 | 250 ($T_{calcd}$ = 650) | 0.0013 | 0.820 | 0.046 | 0.029 | 0.0016 |
| 1848 | 2.5 | 250 | 0.0038 | 0.310 | 0.066 | 0.056 | 0.012 |
| 1850 | 5.8 | 250 | 0.0088 | 0.700 | 0.100 | 0.085 | 0.012 |
| 1818 | 0.60 | Unreduced | 0.0019 | 0.083 | 0.018 | 0.110 | 0.024 |
| 1818 | 0.60 | 250 | 0.0024 | 0.830 | 0.068 | 0.036 | 0.0028 |
| 1827 | 0.58 | Unreduced | 0.0027 | 0.087 | 0.029 | 0.082 | 0.027 |
| 1827 | 0.58 | 250 | 0.0011 | 0.210 | 0.031 | 0.052 | 0.027 |

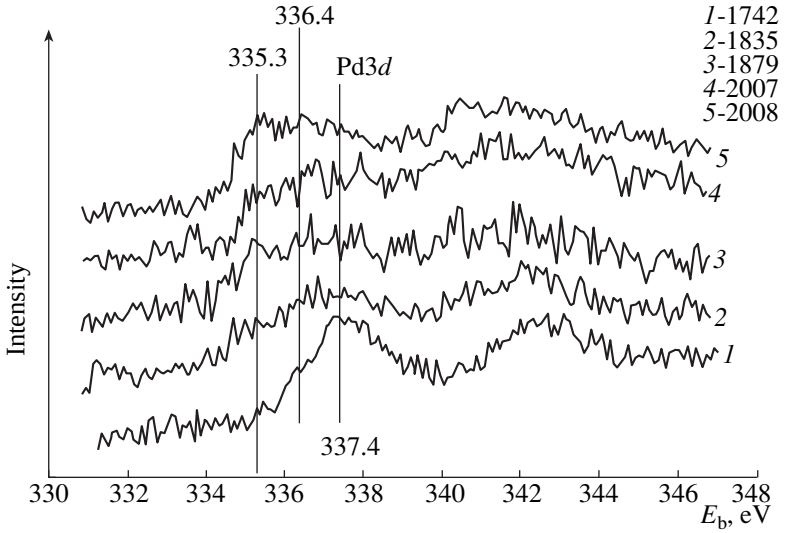


**Fig. 4.** XPS spectra of samples containing 0.5% Pd.

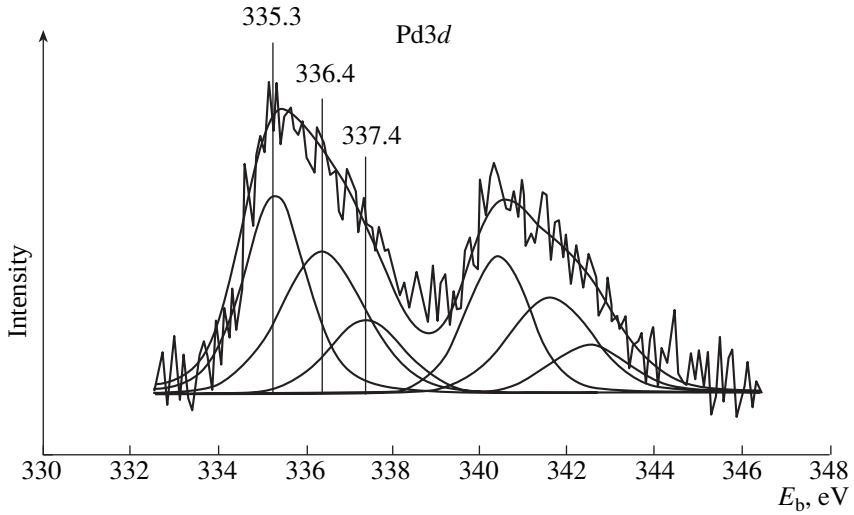


**Fig. 5.** XPS Pd3*d* spectrum of a 0.5 Pd/C catalyst after calcination at 650°C (sample no. 2008) decomposed into individual components.

persed palladium particles in the oxidation state $Pd^+$; that is, electron transfer from palladium to the carbon support took place.

The subsequent reduction of samples in hydrogen at 250 (no. 1835) and 300°C (no. 1879) resulted in a decrease in the peak with $E_b$ = 337.5 eV and in an increase in the peak with $E_b$ = 336.4 eV, which is characteristic of $Pd^+$. Note that the Cl2*p* line intensity in sample no. 1879 somewhat decreased as compared with that in sample no. 1835. Next, the appearance of a small shoulder with the binding energy 335.3 eV, which is characteristic of palladium metal, in the spectra of these samples should be noted; this shoulder was more pronounced in sample no. 1879. A lower intensity of the peak of palladium in reduced samples, as compared with unreduced palladium, suggests that the intercalation of palladium atoms into the interlayer space of graphite or the agglomeration of palladium to form coarser particles, as compared with the initial sample (no. 1742; $PdCl_2$/C after drying), took place in the course of reduction. Note that a portion of palladium with $E_b$ = 337.5 eV was retained after reduction. This is due to the stronger interaction of a portion of palladium chloride with the support. It is reasonable to assume that $Pd^{2+}$ ions are incorporated into the interlayer spaces of graphite.

The calcination of reduced 0.5% Pd/C catalysts at 450 (no. 2007) or even 650°C (no. 2008) for 1 h did not result in considerable agglomeration of palladium; only insignificant Pd redistribution over different valence states was observed (Fig. 5). To determine more accurately the component ratio between metallic and oxi-

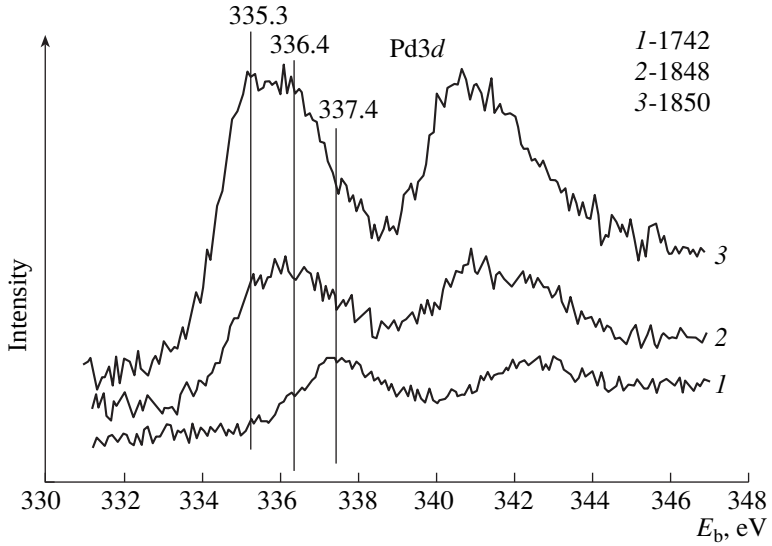


**Fig. 6.** XPS Pd3*d* spectra of a fresh sample (no. 1742 with $PdCl_2$) and reduced Pd/C catalysts with 2 (no. 1848) and 5% (no. 1850) Pd contents.

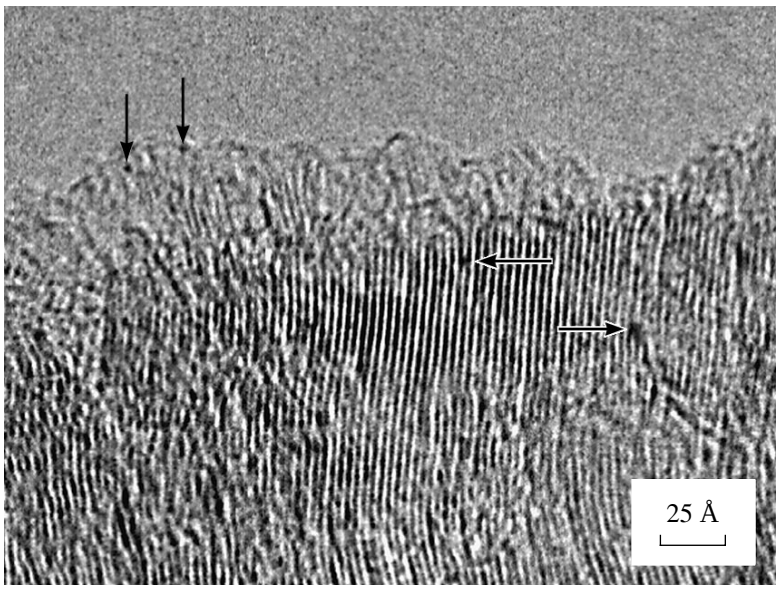


**Fig. 7.** Electron micrograph of a 0.5 wt % Pd/C catalyst (filamentous carbon with the stacklike structure) calcined in an inert gas at 450°C. The arrows indicate contrast dots.

dized palladium, we performed the deconvolution of complex photoelectron spectra into individual peaks (FitXPS program). This thermal stability of Pd/C catalysts is indicative of the strong interaction of palladium with the support. Note that the Pd3*d*/Cl*s* ratio increased; consequently, the amount of palladium on the surface of carbon increased by ~10–20% after heating at 650°C. We explained this fact by the egress of intercalated palladium from the bulk of the support and by agglomeration into $Pd^0$ particles. Table 4 summarizes the ratios between the atomic concentrations of elements in the test samples.

We experimentally found that filamentous carbon with the stacklike structure exhibits the strongest adsorption properties as compared with nanofibers that have the coaxially conical or coaxially cylindrical structure. For example, after etching in aqua regia, considerable amounts of chlorine atoms were present at the surface of all of the three types of filamentous carbon (Table 4). According to XPS data, the concentrations of chlorine atoms in nanofibers changed differently after supporting palladium chloride and the reduction of the samples in a flow of hydrogen at $T = 250$°C. Chlorine was almost absent from the filamentous carbon with the

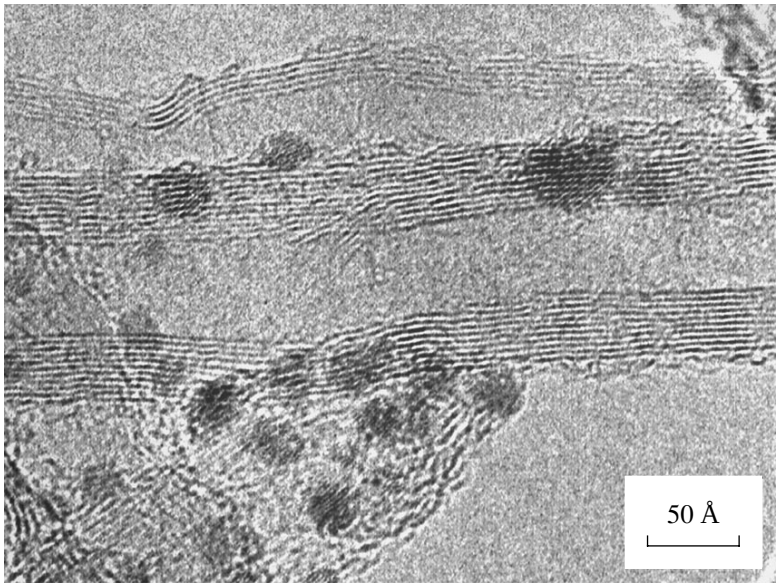


**Fig. 8.** Electron micrograph of a 2 wt % Pd/C catalyst (filamentous carbon with the coaxially cylindrical structure).

coaxially cylindrical structure after the reduction of the sample, whereas the chlorine content of the filamentous carbon with the stacklike structure decreased insignificantly (by a factor of 3 to 4).

The state of palladium can be more clearly identified using Pd/C catalysts with 2.5 (no. 1848) and 5.8% (no. 1850) palladium concentrations (Fig. 6). An analysis of the Pd3*d* spectra of the above samples indicates that after reduction at 250°C palladium occurred in metal ($Pd^0$, 335.3 eV) and oxidized ($Pd^+$, 336.4 eV) states. The fraction of palladium metal in the latter sample was higher. This result is consistent with data on the dispersity of palladium. As Pd concentration in the catalyst was increased from 0.5 to 5.8 wt %, the dispersity of palladium decreased from 33 to 50 Å (Table 5).

**Table 5.** Effect of the properties of carbon supports on the dispersity of Pd/C catalysts*

| Sample no. | Type of filamentous carbon | Palladium content, wt % | Dispersity, Å |
|---|---|---|---|
| 1205 | Stacklike | 0 | – |
| 1835 | Stacklike | 0.5 | 33 |
| 2007** | Stacklike | 0.5 | 70 |
| 2008*** | Stacklike | 0.5 | 70 |
| 1848 | Stacklike | 2.5 | 31 |
| 1850 | Stacklike | 5.8 | 50 |
| 1827 | Coaxially conical | 0.58 | 31 |
| 1841 | Coaxially conical | 3.15 | 73 |
| 1818 | Coaxially cylindrical | 0.60 | 41 |
| 1842 | Coaxially cylindrical | 2.62 | 70 |

* The temperature of reduction was 250°C.
** The temperature of calcination was 450°C.
*** The temperature of calcination was 650°C.

Among the three types of nanofibers, filamentous carbon with the stacklike structure is characterized by the strongest interaction with palladium, which manifests itself in a stronger redistribution of electron density in the palladium–carbon system and in a higher dispersity of Pd. The Pd3*d* spectrum exhibited a shift of the peak (335.3 eV) that corresponds to $Pd^0$ toward higher energies, which are characteristic of oxidized palladium (336.4 eV); this fact is indicative of electron transfer from palladium to carbon.

### *Study of Pd/C Catalysts by High-Resolution Electron Microscopy*

An electron-microscopic study of Pd/C catalysts prepared by supporting ~0.5 wt % Pd on filamentous carbon of coaxially cylindrical, coaxially conical, and stacklike types revealed only very rare palladium particles about 20 Å in size. This fact suggests that palladium primarily occurred in the samples in ionic form and had near-atomic dispersity. Note that, after the calcination of a 0.5 wt % Pd/C sample with the stacklike structure of carbon in argon at 450°C, frequent contrast dots with a size of ~5 Å appeared on the background of the image of graphite planes (Fig. 7). It is likely that palladium in ionic form was reduced with the formation of metal clusters in the cavities of the graphite structure; these clusters gave the contrast observed in the high-resolution electron micrographs. An increase in the palladium content of Pd/C catalysts up to 2 wt %

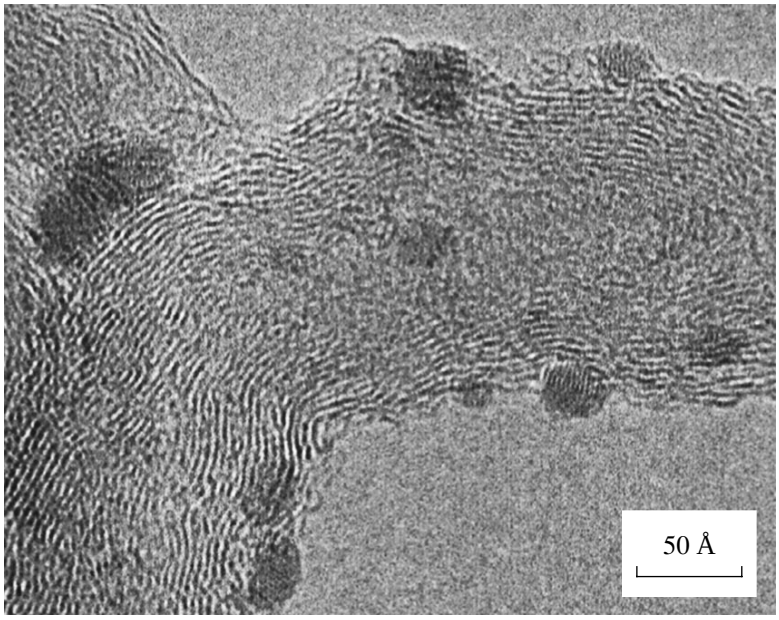


**Fig. 9.** Electron micrograph of a 2 wt % Pd/C catalyst (filamentous carbon with the coaxially conical structure).

resulted in the formation of a great number of particles with a size of 10–40 Å on the surface of filaments with the coaxially conical and coaxially cylindrical structures. Figures 8 and 9 demonstrate the electron micrographs of palladium particles supported on these fibers in catalysts with higher palladium contents. At the same time, we found that metal particles occurred very rarely on filamentous carbon with the stacklike structure, even though the concentration of Pd was increased up to 5 wt %.

### *Catalytic Measurements*

The activity and selectivity of Pd/C catalysts in the reaction of selective 1,3-butadiene hydrogenation to butenes were measured at 60–150°C. The specific catalytic activity of Pd/C catalysts insignificantly increased with temperature; this fact indicates that the activation energy of the hydrogenation reaction is low. Table 6 compares the catalytic activity of Pd/C catalysts at 100°C. It can be seen that Pd/C catalysts in which filamentous carbon with the coaxially cylindrical structure was used as the support exhibited the highest activity. It is likely that this fact can be explained by a lower activity of $Pd^{2+}$ as compared with $Pd^{+}$ and $Pd^{0}$ and by the possible intercalation of a portion of palladium into the bulk of filamentous carbon. The $Pd^{2+}$ content of sample no. 1835 is higher than that of sample nos. 1827 and 1818; therefore, the activity of this sample is higher.

Butane, 1-butene, *cis*-butene, and *trans*-butene were detected in the reaction products of butadiene hydrogenation. The ratios between different butenes remained almost constant. The amounts of 1-butene and *cis*-2-butene were almost equal, and the amount of *trans*-2-butene was greater than that of 1-butene by a factor of 1.5–2.0.

Figure 10 illustrates the effect of carbon support on the selectivity of Pd/C catalysts for butenes in the reaction of butadiene hydrogenation. It is interesting to note that the selectivity for butenes as a function of palladium content passes through a maximum in samples with the coaxially cylindrical and stacklike structures of nanofibers. The selectivity of the Pd/C catalyst increased as the Pd content was decreased from 5.8 to 0.5 wt %. Thus, the reaction selectivity for butenes increased with increasing dispersity of palladium metal particles. However, a further decrease in the palladium content from 0.5 to 0.25 wt % resulted in a decrease in the selectivity. In our opinion, this is due to an increase in the concentration of ionic platinum. Consequently, $Pd^{2+}$ exhibits decreased activity and selectivity in the reaction of selective 1,3-butadiene hydrogenation to butenes.

**Table 6.** Comparison of the specific catalytic activities of Pd/C catalysts in the reaction of selective 1,3-butadiene hydrogenation at 100°C

| Sample no. | Palladium content, wt % | Type of filamentous carbon | Specific catalytic activity, mol $s^{-1}$ (g Pd)$^{-1}$ |
|---|---|---|---|
| 1835 | 0.5 | Stacklike ≡ | $3.1 \times 10^{-2}$ |
| 1827 | 0.58 | Coaxially conical ⋘ | $3.7 \times 10^{-2}$ |
| 1818 | 0.60 | Coaxially cylindrical \|\| | $4.0 \times 10^{-2}$ |

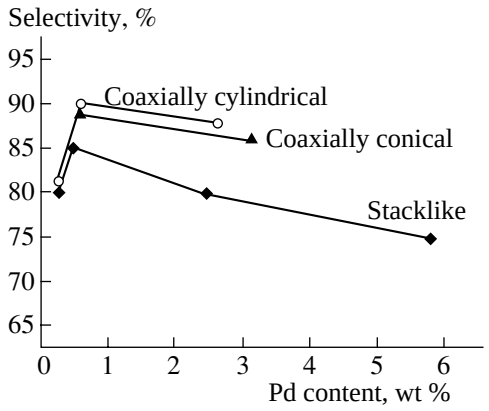


**Fig. 10.** Selectivity of 1,3-butadiene hydrogenation to butenes as a function of the palladium content of Pd/C catalysts.

Thus, we found that the activity and selectivity of Pd/C catalysts in the reaction of selective 1,3-butadiene hydrogenation to butenes depends on the following two factors:

(1) The selectivity increases with increasing dispersity of palladium metal in the same type of filamentous carbon.

(2) An increase in the fraction of $Pd^{2+}$ in the catalysts results in a decrease in both the overall activity and selectivity (at approximately the same dispersity of palladium). The ionic state $Pd^{2+}$ is stabilized by the strong interaction of palladium with the butt-end faces of graphite.

## ACKNOWLEDGMENTS

This work was supported by the Russian Foundation for Basic Research (project no. 00-03-32431) and the program "Leading Scientific Schools of the Russian Federation" (grant no. 00-15-97440).

## REFERENCES

1. Bos, A.N.R. and Westerterp, K.R., *Chem. Eng. Process*, 1993, vol. 32, p. 1.
2. Derrien, D.L., *Stud. Surf. Sci. Catal.*, 1986, vol. 27, p. 613.
3. Boitiaux, J.P., Cosyns, J., and Robert, E., *Appl. Catal.*, 1987, p. 193.
4. Hub, S. and Touroude, R., *J. Catal.*, 1988, vol. 114, p. 411.
5. Murzin, D.Yu., *Khim. Prom-st.*, 1999, no. 1, p. 14.
6. Semikolenov, V.A., *Zh. Prikl. Khim.*, 1997, vol. 70, no. 5, p. 785.
7. Semikolenov, V.A., *Usp. Khim.*, 1992, vol. 61, no. 2, p. 320.
8. Zakarina, N.A. and Zakumbaeva, G.D., *Vysokodispersnye metallicheskie katalizatory* (Highly Dispersed Metal Catalysts), Alma-Ata: Nauka, 1987.
9. Simonov, P.A., Romanenko, A.V., Prosvirin, I.P., Moroz, E.M., Boronin, A.I., Chuvilin, A.L., and Likholovob, V.A., *Carbon*, 1997, vol. 35, no. 1, p. 73.
10. Bertolini, J.C., Delichere, P., Khanra, B.C., Massardier, J., Noupa, C., and Tardy, B., *Catal. Lett.*, vol. 6, p. 215.
11. Chesnokov, V.V. and Buyanov, R.A., *Usp. Khim.*, 2000, vol. 69, no. 7, p. 675.
12. Heal, G.R. and Mkayula, L.L., *Carbon*, 1988, vol. 26, no. 6, p. 815.
13. Moulder, J.F., Stickle, W.F., Sobol, P.E., and Bomben, K.D., *Handbook of X-Ray Photoelectron Spectroscopy*, Chastain, J. and den Prairie, E., Eds., Eden Prairie: Perkin-Elmer, 1992.
14. Shaikhutdinov, Sh.K., Zaikovskii, V.I., and Avdeeva, L.B., *Appl. Catal., A*, 1996, vol. 148, p. 123.
15. Simonov, A.P., Troitskii, S.Yu., and Likholobov, V.A., *Kinet. Katal.*, 2000, vol. 41, no. 2, p. 281.
16. Mason, M.G., *Phys. Rev. B: Condens. Matter*, 1983, vol. 27, p. 748.
17. Kuhrt, Ch. and Harsdorff, M., *Surf. Sci.*, 1991, vol. 245, p. 173.
18. Fritsch, A. and Legare, P., *Surf. Sci.*, 1985, vol. 162, p. 742.
19. Bastl, Z., Piibyl, O., and Mikusik, P., *Czech. J. Phys.*, 1984, vol. 34, p. 981.
20. Vijayakrishnau, V., Chainami, D., Sarme, D.D., and Rao, C.N.R., *J. Phys. Chem.*, 1992, vol. 96, p. 8679.